Research Article | Vol. 29, No. 23 / 8 Nov 2021 / Optics Express 37253
Optics EXPRESS

Pole analysis of EIT-AT spectrum with Rydberg atoms

MENG SHI,[1] YUECHUN JIAO,[2] AND JIANMING ZHAO[2,*]

[1]Key Laboratory of Space Utilization, Technology and Engineering Center for Space Utilization, Chinese Academy of Sciences, Beijing 100094, China
[2]State Key Laboratory of Quantum Optics and Quantum Optics Devices, Institute of Laser Spectroscopy, Shanxi University, Taiyuan 030006, China
*zhaojm@sxu.edu.cn

Abstract: We investigate the electromagnetically induced transparency (EIT) and Autler Townes (AT) splitting spectrum with a four-level Rydberg atom by pole analysis of the probe coherence. A pair of poles corresponding to the two peaks of the spectral splitting is observed. The spectral split or the pole positions are affected by the microwave intensity (MW) and the detuning between the probe and the coupling laser. In the absence of any detuning, the two poles coincide and separate again on the imaginary axis of the complex detuning plane at weak MW field. The two poles do not coincide when the probe (coupling) laser is detuned for scanning the coupling (probe) laser frequency. However, under finite detuning, the two poles approach the nearest distance in the absence of any splitting and are separated again in the direction parallel to the imaginary axis. The spectral analysis of the poles provides an alternate way to establish the relationship between the splitting and the intensity of MW, which may play a role in the application of atomic-based MW measurements.

1. Introduction

Rydberg atom-based microwave (MW) measurement has been successfully developed in the last decade [1–8]. This measurement method is based on the concept of the electromagnetically induced transparency (EIT) and the Autler-Townes (AT) splitting spectrum in a room-temperature vapor cell. The sensitivity of Rydberg atom-based MW measurement reaches 55nV $cm^{-1}Hz^{-1/2}$ with the superheterodyne technique [6], which shows much more precision than traditional measurement devices. It can measure not only the amplitude of MW but also the polarization [2,9], phase [10,11], frequency [12]. Meanwhile, it is an all-optical detector and can be very small in dimension using the micro vapor cell. The setup has many advantages over conventional MW measurement devices, for example, antenna wire [13]. The Rydberg atom-based MW measurement has many applications, such as radar, radio frequency receiver, MW communication, astronomical measurement, etc. The high precision of a MW measurement depends on the linear relation between the fine splitting of AT spectrum and the intensity of MW, $|E| = \frac{\hbar}{\mu}\Omega_{MW} = 2\pi\frac{\hbar}{\mu}\Delta f$, where Δf is the splitting in AT spectrum, $\hbar$ is Planck's constant, and Ω_{MW} and μ are Rabi frequency and atomic dipole moments between two Rydberg states [1]. However, the linear relation is invalid within a small intensity regime, and the splitting disappears before the microwave intensity decreases to zero [14]. Therefore, there always exists a threshold intensity at which one cannot measure the weak MW by the EIT-AT splitting method. Within this limit, it is also hard to distinguish between the EIT effect and the AT effect, as both of the effects are equally dominant [15,16]. As the intensity of MW decreases, the dominant effect changes from AT splitting to EIT effect gradually [15]. There is a way to avoid this nonlinear area for detecting weak MW by adding a known strong MW [6,17]. However, the spectral splitting within the weak intensity regime still needs to be investigated.

#440103 https://doi.org/10.1364/OE.440103
Journal © 2021 Received 11 Aug 2021; revised 14 Oct 2021; accepted 15 Oct 2021; published 26 Oct 2021

Optics EXPRESS

In this work, we study the AT splitting with MW intensity by analyzing poles of the denominator of the probe coherence, which is a very useful method of studying resonances in scattering theory [18]. Similar pole analysis on a three-level atomic system was conducted in Ref. [19], which is successfully used to analyze the position and width of the peak on the absorption spectrum. By analyzing the probe coherence of a four-level atomic system in our paper, we found three poles by scanning the probe laser and two poles by scanning the coupling laser [14,20]. A pair of poles symmetrically lay on the complex detuning plane for probe laser and coupling laser, respectively. The distance between the two poles correspond to the splitting of the EIT-AT spectrum as a function of the MW field is investigated. When the intensity of MW decreases to a critical value, the splitting disappears. The two poles overlap or get closer. After that, the two poles separate again in the vertical direction, and there is only one peak on the spectrum. The detuning of one of the lasers also changes the behavior of the two poles while scanning the other laser. It brings a more ideal way to investigate the AT splitting and the intensity of MW. The experiment will be conducted further.

2. Probe coherence of the four-level Rydberg atom

The MW measurement with the AT splitting effect is based on a four-level system of Rydberg atom. The typical setup is shown in Fig. 1(a). A probe laser and a coupling laser go through a vapor cell in the opposite direction. The photodetector receives the spectrum signal from the probe laser by scanning the frequency of the probe laser or coupling laser. The Rydberg atom is excited by the two lasers, shown as in Fig. 1(b), forming a cascade three-level EIT atomic system. For the ^{133}Cs four energy levels, for example, MW field generated from a horn couples two Rydberg states $52D_{5/2}$ and $53P_{3/2}$, corresponding Rydberg EIT spectrum would split into two peaks due to MW dressed AT splitting. The four states in Fig. 1(b) are denoted as $|1\rangle$, $|2\rangle$, $|3\rangle$ and $|4\rangle$ from the bottom to the top.

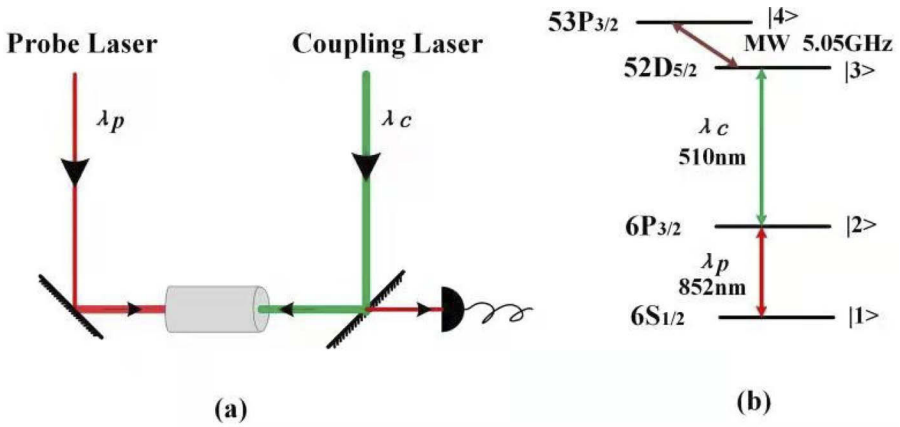

Fig. 1. Rydberg atom excitation by two laser and coupling with a MW field for experimental setup (a) and related four-level system (b).

The atom population in the four-ladder system is usually solved by the density matrix equation, and it is shown as [20]

$$\frac{\partial \rho}{\partial t} = -\frac{i}{\hbar}[H, \rho] + L', \tag{1}$$

where H is the Hamiltonian, and L' is the Lindblad operator corresponding to the decay process of excited atoms.

Optics EXPRESS

Considering the rotating wave approximation, the Hamiltonian for the four-level system is given as

$$H = \begin{bmatrix} 0 & \Omega_p & 0 & 0 \\ \Omega_p & -2\Delta_p & \Omega_c & 0 \\ 0 & \Omega_c & -2(\Delta_p + \Delta_c) & \Omega_{MW} \\ 0 & 0 & \Omega_{MW} & -2(\Delta_p + \Delta_c + \Delta_{MW}) \end{bmatrix}, \tag{2}$$

where $\Delta_{p,c,MW}$ represent the detuning of the probe laser, coupling laser, and the MW, respectively. $\Omega_{p,c,MW}$ are the Rabi frequency of the probe laser, coupling laser, and the MW, respectively. The L' operator is given by

$$L' = \begin{bmatrix} \Gamma_2\rho_{22} & -\gamma_{12}\rho_{12} & -\gamma_{13}\rho_{13} & -\gamma_{14}\rho_{14} \\ -\gamma_{21}\rho_{21} & \Gamma_3\rho_{33} - \Gamma_2\rho_{22} & -\gamma_{23}\rho_{23} & -\gamma_{24}\rho_{24} \\ -\gamma_{31}\rho_{31} & -\gamma_{32}\rho_{32} & \Gamma_4\rho_{44} - \Gamma_3\rho_{33} & -\gamma_{34}\rho_{34} \\ -\gamma_{41}\rho_{41} & -\gamma_{42}\rho_{42} & -\gamma_{43}\rho_{43} & -\Gamma_4\rho_{44} \end{bmatrix}, \tag{3}$$

where $\gamma_{ij} = (\Gamma_i + \Gamma_j)/2$, and Γ_i is the decay rate of the excited state. For ^{133}Cs, the ground state $6S_{1/2}$ has $\Gamma_1 = 0$, the excited states are set with $\Gamma_2 = 2\pi \times 6$ MHz, $\Gamma_3 = 2\pi \times 3$ kHz, $\Gamma_2 = 2\pi \times 2$ kHz.

Under the assumption of weak probe laser, $\Omega_p << \Gamma_2, \Omega_c$, we can neglect the second order in Ω_p and solve Eq. (1) in the steady state. The solution of ρ_{21}, the transition of state $|2\rangle$ to state $|1\rangle$, is derived as [14],

$$\rho_{21} = \frac{\Omega_p}{2} \frac{1}{\Delta_p - i\gamma_{21} + \frac{\Omega_c^2(\Delta_p + \Delta_c + \Delta_{MW} - i\gamma_{41})}{\Omega_{MW}^2 - 4(\Delta_p + \Delta_c - i\gamma_{31})(\Delta_p + \Delta_c + \Delta_{MW} - i\gamma_{41})}}, \tag{4}$$

Here we ignore the Doppler broadening of the energy shift of atoms. We define $d_2 = \Delta_p - i\gamma_{21}$, $d_3 = \Delta_p + \Delta_c - i\gamma_{31}$, $d_4 = \Delta_p + \Delta_c + \Delta_{MW} - i\gamma_{41}$, where $\Delta_{i=p,c,MW}$ are the detuning of probe laser, coupling laser and MW, respectively. To simplify the analysis, we assume Δ_{MW} is zero, ρ_{21} is simplified to

$$\rho_{21} = \frac{\Omega_p}{2} \frac{\Omega_{MW}^2 - 4d_3d_4}{d_2\Omega_{MW}^2 - 4d_2d_3d_4 + d_4\Omega_c^2}. \tag{5}$$

It is seen that the dominator contains three orders of the Δ_p and two orders of the Δ_c. Therefore, there are three poles for scanning probe laser and two poles for scanning the coupling laser.

3. Pole moving with the intensity of MW

There are two ways to observe the AT spectrum by scanning the probe laser or coupling laser frequency, respectively. However, since the detuning of Δ_p and Δ_c are asymmetric in the probe coherence ρ_{21}, the spectra have differences at the shoulders, as shown in Fig. 2.

It can be seen that the splitting is the same for scanning probe laser and coupling laser. The difference is the shoulders of the absorption spectrum. The shoulders of absorption spectrum for the scanning coupling laser saturate, while reduce for the scanning probe laser.

Meanwhile, the denominator of ρ_{21} has different order polynomials for the detuning parameters Δ_p and Δ_c. For the case of scanning the probe laser frequency, the denominator is the triple-order

Optics EXPRESS

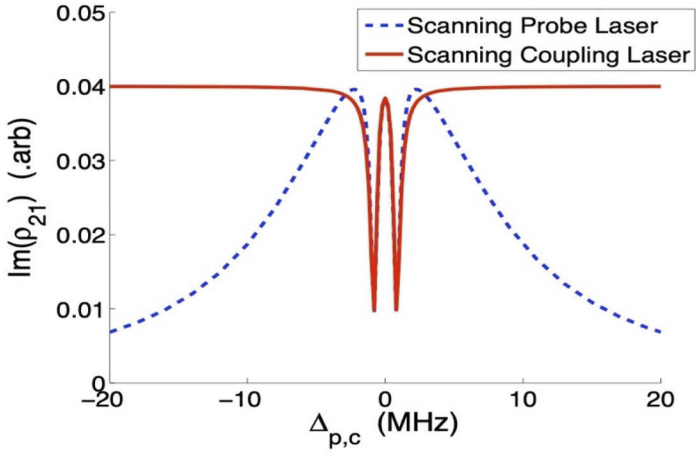

Fig. 2. The spectra of scanning the probe laser frequency (blue) and the coupling laser frequency (red) at $\Omega_{MW} = 2\pi \times 1.6$ MHz.

polynomial of Δ_p. Therefore, there are three poles, and ρ_{21} can be expressed as

$$\rho_{21} = \frac{\Omega_p}{2} \frac{d_3 d_4 - \Omega_{MW}^2/4}{(\Delta_p - \delta_{p1})(\Delta_p - \delta_{p2})(\Delta_p - \delta_{p3})}, \tag{6}$$

and δ_{p1}, δ_{p2}, δ_{p3} are same as Ref. [14],

$$\begin{aligned}
\delta_{p1} &= \frac{1}{3}\left(d + 2^{\frac{1}{3}}\frac{L_1}{L_3} - 2^{-\frac{1}{3}}L_3\right), \\
\delta_{p2} &= \frac{1}{3}\left(d - 2^{-\frac{1}{3}}\left(1 + i\sqrt{3}\right)\frac{L_1}{L_3} + 2^{-\frac{4}{3}}\left(1 - i\sqrt{3}\right)L_3\right), \\
\delta_{p3} &= \frac{1}{3}\left(d - 2^{-\frac{1}{3}}\left(1 - i\sqrt{3}\right)\frac{L_1}{L_3} + 2^{-\frac{4}{3}}\left(1 + i\sqrt{3}\right)L_3\right),
\end{aligned} \tag{7}$$

where

$$\begin{aligned}
d &= -(t_2 + t_3 + t_4), \\
L_1 &= -t_2^2 + t_2 t_3 - t_3^2 + t_2 t_4 + t_3 t_4 - t_4^2 - 3\Omega_c^2 - 3\Omega_{MW}^2, \\
L_2 &= 2t_2^3 - 3t_2^2 t_3 - 3t_3^2 t_2 - 3t_2^2 t_4 - 3t_3^2 t_4 - 3t_4^2 t_2 - 3t_4^2 t_3 \\
&\quad + 2t_3^3 + 12 t_2 t_3 t_4 + 2t_4^3 + 9t_2\Omega_c^2 + 9t_3\Omega_c^2 + 9t_3\Omega_{MW}^2 \\
&\quad + 9t_4\Omega_{MW}^2 - 18t_2\Omega_{MW}^2 - 18t_4\Omega_{MW}^2, \\
L_3 &= \left(L_2 + \sqrt{4L_1^2 + L_2^2}\right)^{1/3},
\end{aligned} \tag{8}$$

where $t_2 = d_2(\Delta_p = 0)$, $t_3 = d_3(\Delta_p = 0)$, $t_4 = d_4(\Delta_p = 0)$. When there is no detuning, the spectrum and poles move with the intensity of the MW. There always exists a critical power of MW at which one cannot distinguish the splitting since the two peaks merge into one peak when scanning the probe laser frequency.

Optics EXPRESS

For the case of scanning the coupling laser frequency, the denominator is a second-order polynomial of Δ_c. There are two poles, and ρ_{21} can be expressed as

$$\rho_{21} = \frac{\Omega_p}{2d_2} \frac{d_3 d_4 - \Omega_{MW}^2/4}{(\Delta_c - \delta_{c1})(\Delta_c - \delta_{c2})}, \tag{9}$$

where

$$\delta_{c1,c2} = \frac{1}{2}\left(-r_3 - r_4 + \frac{1}{4d_2}\Omega_c^2 \pm \sqrt{\left(r_3 - r_4 - \frac{1}{4d_2}\Omega_c^2\right)^2 + \Omega_{MW}^2}\right), \tag{10}$$

where $r_3 = d_3(\Delta_c = 0)$, $r_4 = d_4(\Delta_c = 0)$.

As shown in Fig. 3(a), it is clearly seen that there are two poles symmetrically distributed on the upper of the complex Δ_p plane, and the third pole lay on the imaginary axis of the Δ_p plane when we scan the probe laser. When we scan the coupling laser, there are two poles symmetrically located on the complex upper of Δ_c plane, as shown in Fig. 3(b). The distance between two poles corresponds to the splitting of the EIT-AT spectrum as in Fig. (2), and the imaginary part of the poles corresponds to the widths of the splitting peaks which are quite familiar with the scattering theory [18].

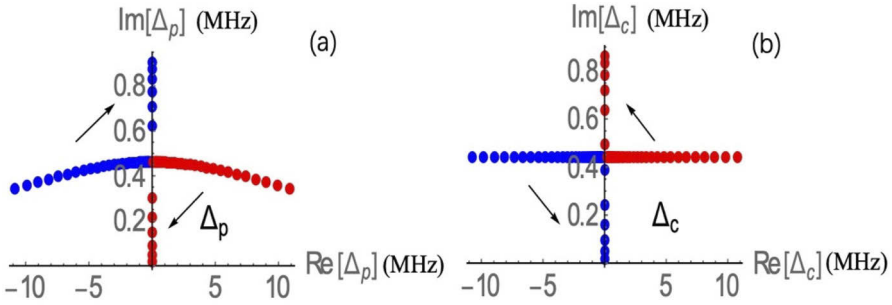

Fig. 3. Pole positions with different MW intensities. The pair of poles on Δ_p plane (a) and on Δ_c plane (b). The arrow means the direction of poles moving as the intensity of MW decreasing.

The pole positions are determined by Δ_p, Δ_c, Ω_c, and Ω_{MW}. We choose $\Omega_c = 2\pi \times 6$ MHz. We set $\Delta_c = 0$ for scanning probe laser, set $\Delta_p = 0$ for scanning coupling laser. Therefore, the pole positions are only determined by Ω_{MW}, therefore the splitting of the spectra are determined by Ω_{MW} as well. It is noted that the Doppler effect will affect the EIT linewidth and further the EIT amplitude for EIT resonances [21,22], but it has negligible effect on the pole positions as Ω_{MW} varies. To simplify the analysis of poles of probe coherence ρ_{21}, we ignore the Doppler effect in the following.

As the intensity of MW decreases, i.e., Ω_{MW} decrease from 20 MHz to 0.15 MHz, the splitting of the AT spectrum decreases. As shown in Fig. 4. The two pairs of poles on the Δ_p and Δ_c get close to each other. When the two peaks merge to one peak, the two pairs of poles meet on the upper section of the imaginary axis of Δ_p and Δ_c, respectively. The meeting points are (0, 0.45) and (0, 0.44) for Δ_p and Δ_c in Fig. 3, which correspond to $\Omega_{MW} = 2\pi \times 0.88$ MHz and $\Omega_{MW} = 2\pi \times 0.86$ MHz in Fig. 4, respectively. The tiny difference of the poles' position is from the different denominator for Δ_p and Δ_c. The third pole on the Δ_p plane always stays at (0,18). It is observed that the third pole changes very little (less than 0.1% of its module), as the intensity of MW changes, which is a nearly stationary point. Therefore, the third pole is only contributed to the background of the AT spectrum. When the intensity of MW decreases further, the AT splitting disappears, and there is only one peak on the spectrum. The EIT effect

Optics EXPRESS

is dominant below this MW intensity [15]. The two pairs of poles separate again but lie on the imaginary axis of Δ_p and Δ_c, respectively. The height of the peak will change as the intensity of MW decreasing. However, the physical meaning between the height of the peak and the two poles on the imaginary axis of Δ_p and Δ_c plane should be studied further.

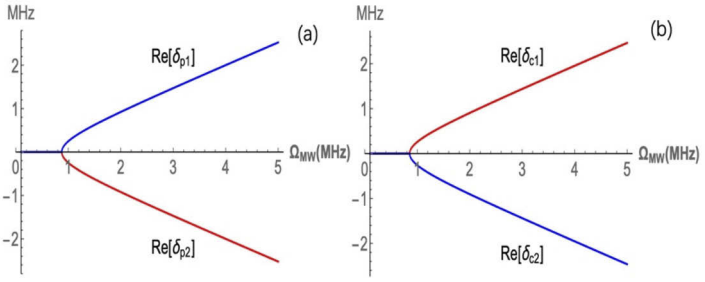

Fig. 4. Real part of pole positions varies with MW intensity. The pair of poles on Δ_p plane (a), and on Δ_c plane (b).

The difference between the poles on Δ_p plane and Δ_c plane is the moving direction after their separation from the meeting point. The right pole on the Δ_p plane moves up after the separation, while the left pole moves down. The poles on the Δ_c plane has the opposite moving direction to that of Δ_p plane.

The spectrum will shift if probe or coupling is detuned, and the calculated result is shown in Fig. 5, with $\Omega_{MW} = 2\pi \times 8$ MHz. For the case of scanning probe laser and coupling laser detuning $\Delta_c = 2\pi \times 0.5$ MHz, the spectrum is shown in Fig. 5(a). The two peaks shift left about 0.5 MHz with the splitting being the same as zero detuning. For the case of scanning the coupling laser, and the detuning of probe laser $\Delta_p = 2\pi \times 0.5$ MHz, the spectrum is shown in Fig. 5(b). Two peaks shift left about 0.5 MHz as well.

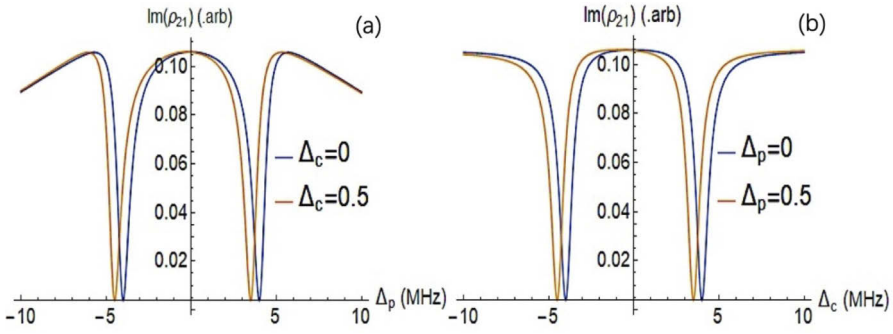

Fig. 5. Effect of the detuning of probe laser and coupling laser on spectra. (a) the spectrum with scanning probe laser, and (b) the spectrum with scanning coupling laser.

The pole positions are also affected by the detuning, as shown in Fig. 6. The detuning are set to $\Delta_p = 2\pi \times 0.2$MHz and $\Delta_c = 2\pi \times 0.2$MHz for probe laser and coupling laser, respectively. The two pairs of poles would not meet each other as the intensity of MW decreases. On Δ_p plane in Fig. 6(a), the two poles have the same imaginary value, but the real parts are symmetric to $(-0.2, 0.46)$. When MW decreases, i.e., Ω_{MW} decrease from 10.0 MHz to 0.4 MHz, the two poles get closer to each other but turn to separate again near the imaginary part. They do not meet like the $\Delta_p = 0$ scenario. The third pole still stays at (0,18) and changes less than 0.1%.

Optics EXPRESS

On the Δ_c plane in Fig. 6(b), the situation is similar, but the poles move in opposite direction comparing with the poles on Δ_p plane. The symmetric center point is (−0.2, 0.44).

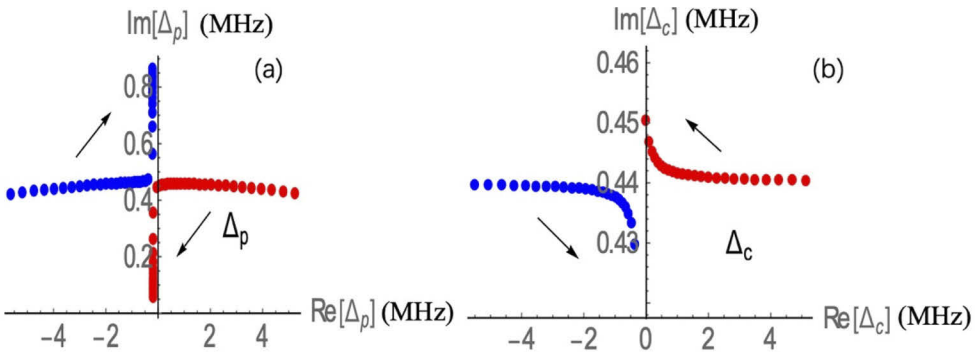

Fig. 6. Pole positions with detuning of probe laser $\Delta_p = 2\pi \times 0.2$MHz (a) and coupling laser $\Delta_c = 2\pi \times 0.2$MHz (b), respectively. The arrow means the direction of poles moving as the intensity of MW decreasing.

When the detuning changes from positive to negative, the symmetric center points for Δ_p and Δ_c plane also change. As shown in Fig. 7(a), when $\Delta_c = -2\pi \times 0.2$ MHz and the other parameters are the same as Fig. 6, the symmetric center point on Δ_p plane moves right to (0.2, 0.46). The poles also move in opposite direction comparing to the case of $\Delta_c = 2\pi \times 0.2$ MHz in Fig. 6(a). As shown in Fig. 7(b), when $\Delta_p = -2\pi \times 0.2$ MHz, the symmetric center point on Δ_c plane moves right to (0.2, 0.44). The poles have different moving behavior compared with the case of $\Delta_p = 2\pi \times 0.2$ MHz as well.

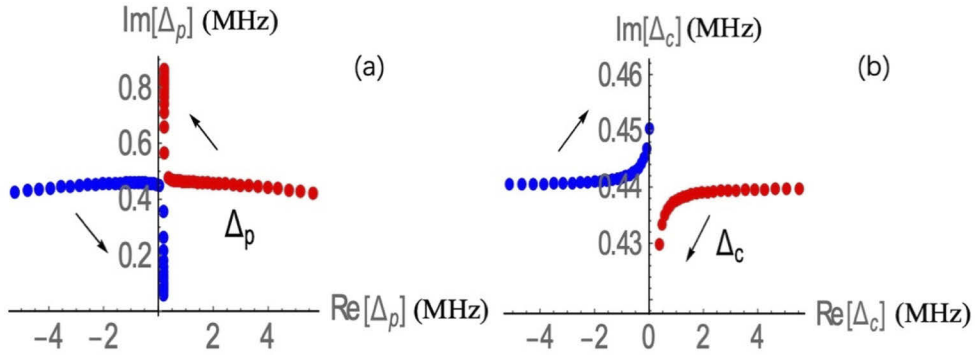

Fig. 7. Pole positions with detuning of the probe laser $\Delta_p = -2\pi \times 0.2$MHz (a) and coupling laser $\Delta_c = -2\pi \times 0.2$MHz (b), respectively. The arrow means the direction of poles moving as the intensity of MW decreasing.

It can be concluded that when the detuning is positive, the symmetrical point on Δ_p and Δ_c plane moves left; otherwise, it moves right. The moving direction of poles is also associated with the sign of detuning. The symmetric center point means the threshold intensity of MW that can be detectable. Below that value, the two poles have the same real part, and the spectrum has only one peak and the splitting disappears. Therefore, the pole analysis provides a more intuitionistic way to find the threshold intensity of the detectable MW and may play a role in the application of atomic-based MW measurements.

Optics EXPRESS

4. Conclusion

A four-ladder type of Rydberg atom excitation can be used to measure MW field. EIT-AT spectrum is the direct way to measure the MW. There are two ways to realize the EIT-AT spectrum by scanning the probe or the coupling laser frequency. However, there is a threshold intensity of MW that the splitting of the EIT-AT spectrum disappears. Through pole analysis, the two peaks correspond to a pair of poles symmetrically laying on the complex Δ_p plane and Δ_c plane. The two poles move on the planes as the intensity of MW changes. Meanwhile, the detuning of the probe laser and the coupling laser also affect the poles' position. The behavior of poles' position at a small intensity of MW needs to be studied further, as it is associated with distinction between the EIT and AT effect. The pole analysis of the EIT- AT spectrum in this work provides a more insightful way to show the relation between the spectrum and the intensity of MW.

Funding. National Natural Science Foundation of China (61601017, 61775124, 11804202, 62175136, 61835007).

Disclosures. The authors declare that there are no conflicts of interest related to this article.

Data availability. Data underlying the results presented in this paper are not publicly available at this time but may be obtained from the authors upon reasonable request.

References

1. J. A. Sedlacek, A. Schwettmann, H. Kübler, R. Löw, T. Pfau, and J. P. Shaffer, "Microwave electrometry with Rydberg atoms in a vapour cell using bright atomic resonances," Nat. Phys. **8**(11), 819–824 (2012).
2. H. Fan, S. Kumar, J. Sedlacek, H. Kübler, S. Karimkashi, and J. P. Shaffer, "Atom based RF electric field sensing," J. Phys. B: At., Mol. Opt. Phys. **48**(20), 202001 (2015).
3. C. L. Holloway, M. T. Simons, J. A. Gordon, A. Dienstfrey, D. A. Anderson, and G. Raithel, "Electric field metrology for SI traceability: Systematic measurement uncertainties in electromagnetically induced transparency in atomic vapor," J. Appl. Phys. **121**(23), 233106 (2017).
4. D. H. Meyer, K. C. Cox, F. K. Fatemi, and P. D. Kunz, "Digital communication with Rydberg atoms and amplitude-modulated microwave fields," Appl. Phys. Lett. **112**(21), 211108 (2018).
5. J. B. Fan, L. P. Hao, Y. M. Xue, J. M. Zhao, and S. T. Jia, "Microwave electromagnetically induced transparency and Aulter-Townes spectrum of cesium Rydberg atom," Acta Physica Sinica **67**(9), 093201 (2018).
6. M. Jing, Y. Hu, J. Ma, H. Zhang, L. Zhang, L. Xiao, and S. Jia, "Atomic superheterodyne receiver based on microwave-dressed Rydberg spectroscopy," Nat. Phys. **16**(9), 911–915 (2020).
7. D. H. Meyer, Z. A. Castillo, K. C. Cox, and P. D. Kunz, "Assessment of Rydberg atoms for wideband electric field sensing," J. Phys. B: At., Mol. Opt. Phys. **53**(3), 034001 (2020).
8. D. H. Meyer, P. D. Kunz, and K. C. Cox, "Waveguide-Coupled Rydberg Spectrum Analyzer from 0 to 20 GHz," Phys. Rev. Appl. **15**(1), 014053 (2021).
9. J. A. Sedlacek, A. Schwettmann, H. Kübler, and J. P. Shaffer, "Atom-Based Vector Microwave Electrometry Using Rubidium Rydberg Atoms in a Vapor Cell," Phys. Rev. Lett. **111**(6), 063001 (2013).
10. M. T. Simons, A. H. Haddab, J. A. Gordon, and C. L. Holloway, "A Rydberg atom-based mixer: Measuring the phase of a radio frequency wave," Appl. Phys. Lett. **114**(11), 114101 (2019).
11. C. L. Holloway, M. T. Simons, J. A. Gordon, and D. Novotny, "Detecting and Receiving Phase Modulated Signals with a Rydberg Atom-Based Mixer," IEEE Antennas and wireless propagation letters **18**(9), 1853–1857 (2019).
12. J. A. Gordon, M. T. Simons, A. H. Haddab, and C. L. Holloway, "Weak electric-field detection with sub-1 Hz resolution at radio frequencies using a Rydberg atom-based mixer," AIP Adv. **9**(4), 045030 (2019).
13. M. T. Simons, J. A. Gordon, and C. L. Holloway, "Fiber-coupled vapor cell for a portable Rydberg atom-based radio frequency electric field sensor," Appl. Opt. **57**(22), 6456–6460 (2018).
14. K. Y. Liao, H. T. Tu, S. Z. Yang, C. J. Chen, X. H. Liu, J. Liang, X. D. Zhang, H. Yan, and S. L. Zhu, "Microwave electrometry via electromagnetically induced absorption in cold Rydberg atoms," Phys. Rev. A **101**(5), 053432 (2020).
15. Z. Ji, Y. Jiao, Y. Xue, L. Hao, J. Zhao, and S. Jia, "Distinction of electromagnetically induced transparency and Autler-Towners splitting in a Rydberg-involved ladder-type cold atom system," Opt. Express **29**(8), 11406–11415 (2021).
16. T. Y. Abi-Salloum, "Electromagnetically induced transparency and Autler-Townes splitting: Two similar but distinct phenomena in two categories of three-level atomic systems," Phys. Rev. A **81**(5), 053836 (2010).
17. L. Hao, Y. Xue, J. Fan, J. Bai, Y. Jiao, and J. Zhao, "Precise measurement of a weak radio frequency electric field using a resonant atomic probe," Chin. Phys. B **29**(3), 033201 (2020).
18. J. R. Taylor, *Scattering theory* (John Wiley & Sons, Ltd, 1972).
19. G. Vemuri, G. S. Agarwal, and B. D. Nageswara Rao, "Sub-Doppler resolution in inhomogeneously broadened media using intense control fields," Phys. Rev. A **53**(4), 2842–2845 (1996).

Optics EXPRESS

20. H. S. Rawat, S. K. Dubey, and V. N. Ojha, "Distinction between double electromagnetically induced transparency and double Autler–Townes splitting in RF-driven four-level ladder 87Rb atomic vapor," J. Phys. B: At., Mol. Opt. Phys. **51**(15), 155401 (2018).
21. A. Javan, O. Kocharovskaya, H. Lee, and M. O. Scully, "Narrowing of electromagnetically induced transparency resonance in a Doppler-broadened medium," Phys. Rev. A **66**(1), 013805 (2002).
22. B. C. Das, D. Bhattacharyya, A. Das, S. Saha, S. Chakrabarti, and S. De, "Pulse delay and group velocity dispersion measurement in V-type electromagnetically induced transparency of hot 85Rb atom," J. Phys. B: At., Mol. Opt. Phys. **51**(24), 245501 (2018).